Research Square

Preprints are preliminary reports that have not undergone peer review.
They should not be considered conclusive, used to inform clinical practice,
or referenced by the media as validated information.

Unlocking Glutamate Dynamics: The Potential of the Glutamate-Binding Protein from Corynebacterium glutamicum as a Fluorescence Probe in Cerebrospinal Fluid Analysis

GIOVANNI FERRARA
Institute of Food Science
Antonio Varriale
Institute of Food Science
Ivana Milosevic
BioSense Institute
Vasa Radonic
BioSense Institute
Sabato D'Auria
sabato.dauria@cnr.it

Institute of Food Science
Maria Staiano
Institute of Food Science

Article

Keywords: Fluorescence, Glutamate, Glutamate-binding protein, Biosensor, Proteins

Posted Date: September 22nd, 2026

DOI: https://doi.org/10.21203/rs.3.rs-10640797/v1

License: This work is licensed under a Creative Commons Attribution 4.0 International License.
Read Full License

Additional Declarations: No competing interests reported.

Version of Record: A version of this preprint was published at Scientific Reports on November 13th, 2026. See the published version at https://doi.org/10.1038/s41598-026-80347-x.

Abstract

L-Glutamate (L-Glu) is the primary excitatory neurotransmitter in the mammalian central nervous system. In neurobiology, monitoring L-Glu accumulation is critical to track the neurodegeneration process, since excessive extracellular levels are caused by acute events like stroke, brain injuries, or malignant tumors. Conventional analytical methods are widely used to quantify L-Glu. Recently, alternative approaches based on biosensors have been developed for monitoring L-Glu in biological systems. In this work, we explored the use of the glutamate-binding protein (GluB), isolated from *Corynebacterium glutamicum*, as a specific probe to design a fluorescence biosensor for L-Glu detection. For this purpose, one of the three cysteine residues of GluB was labeled with the environment-sensitive fluorescence dye acrylodan. The stability of the labeled protein was assessed through thermal stability experiments. The binding of L-Glu to the GluB-acrylodan was investigated by steady-state and time-resolved fluorescence measurements.

The results indicate the capability of the biosensor to effectively intercept the concentration values of L-Glu that are characteristic of acute clinical emergencies and tumor microenvironments before they can reach extreme neurotoxic levels. To explore the clinical potential application of the assay, GluB-acrylodan was tested through time-resolved fluorescence measurements in artificial cerebrospinal fluid (aCSF). The results showed a LoD of 310 μM, a threshold value that is compatible with the pathological concentrations of L-Glu, confirming that GluB-acrylodan is a promising analytical tool in neurobiological research, clinical monitoring and cellular excitotoxic events.

1. Introduction

L-Glutamate (L-Glu) is the primary excitatory neurotransmitter in the mammalian central nervous system, playing a fundamental role in synaptic plasticity, learning, and memory [1]. Consequently, maintaining glutamate homeostasis is crucial for cells [2]. Excessive extracellular glutamate levels cause excitotoxicity, leading to neuronal death and neurodegenerative diseases such as Alzheimer's, Parkinson's, and Amyotrophic Lateral Sclerosis (ALS) [3].

The use of L-Glu has also found application in the food industry, usually as monosodium glutamate (MSG),to improve food flavor [4]. MSG activates taste receptors, improving the natural taste and texture of foods, enhancing thickness, fullness, and mildness of flavor [5, 6]. However, the use of MSG has raised concerns about its potential effects on health [7]. In some people, high intake of MSG has been associated with adverse reactions such as headache, sweating, and nausea [8].

In neurobiology, monitoring the concentration of extracellular L-Glu is a challenge due to the gap between physiological events and pathological conditions [9, 10]. During normal synaptic transmission, L-Glu transiently rises to approximately 1.0 mM within the synaptic cleft, and it is rapidly cleared within a few milliseconds [11]. Abnormal cellular conditions can lead to an accumulation of the neurotransmitter that can induce neurodegeneration processes [12].

For example, during ischemic stroke or traumatic brain injury, the loss of homeostasis increases the extracellular levels of L-Glu into micromolar or millimolar concentration range [13].

Similarly, within the microenvironment of malignant brain tumors like glioblastomas, cells secrete L-Glu, contributing to raising local concentration values of L-Glu above 500 μM [14, 15].

It appears necessary to have an analytical system capable of detecting the presence of L-Glu at the concentrations found in excitotoxicity and track acute clinical events [16, 17].

Biosensors have been mainly developed for monitoring L-Glu in biological systems and for food quality control [18–20] as an alternative to the conventional analytical methods [21, 22].

In recent years, protein-based biosensors have emerged as a promising alternative due to their high specificity and affinity towards the target analyte, contributing to overcome the disadvantages of conventional methods (sampling, pretreatment) [23, 24]. Specifically, periplasmic binding proteins (PBPs), belonging to the ABC-transporter superfamily, have gained attention for the design of new protein-based biosensors [25–28].

The proteins belonging to this family share a common characteristic structural architecture. Their tertiary structure is composed of two main globular domains that are connected by a flexible hinge region. Upon ligand binding, the protein undergoes a conformational transition from an open solvent-exposed conformation to a compact closed conformation [20, 29, 30]. This conformational shift can generate an optical variation that we can utilize to monitor the presence of binding substrate events.

Among the fluorescence probes, acrylodan (6-acryloyl-2-dimethylaminonaphthalene) is a well-known sensitive environment-responsive probe, widely utilized in sensing applications due to its high sensitivity to local environment variations [31]. In fact, it responds to sensitive structural protein changes when it is located near the substrate binding site, or it is close to a hinge region [32].

In the case of the PBPs, upon ligand binding, the acrylodan moves from a solvent-exposed micro-environment to a shielded and hydrophobic one, causing a variation of the fluorescence features of the dye that can be monitored by fluorescence spectroscopy techniques. This approach has been implemented in several PBP-based systems [33], highlighting the use of acrylodan in sensing-protein-based applications.

In this work, we explored the use of the glutamate-binding protein (GluB), isolated from *Corynebacterium glutamicum* [34] for the design of a fluorescence assay for L-Glu detection. We labeled one of the three cysteine residues of GluB with acrylodan and studied the effects of L-Glu binding to GluB on variations of the fluorescence properties of acrylodan. In addition, to verify if the acrylodan labeling procedure could affect the protein stability, thermal studies were performed on GluB in the absence and in the presence of increasing concentrations of L-Glu.

The results show that the acrylodan-labeled GluB stability is only barely affected by the labeling procedure at high temperature (50°C). The labeled GluB is still able to bind L-Glu with a good affinity. To explore the analytical relevance of GluB-acrylodan in physiological matrices, time-resolved fluorescence measurements were successfully validated in artificial cerebrospinal fluid (aCSF).

2. Results and Discussion

2.1 GluB-acrylodan thermal stability analysis

The evaluation of the effect of the presence of a fluorescence probe on the structural properties of GluB is a crucial step before using this protein to design a biosensor for L-Glu detection. For this purpose, thermal stability experiments were conducted on GluB-acrylodan at 25°C and 50°C, in the absence and in the presence of L-Glu.

Figure 1a and Fig. 1b show the time-dependent variations of the maximum fluorescence intensity emission of GluB and GluB-acrylodan in the absence and in the presence of L-Glu upon incubation at 25°C, respectively. It is possible to conclude that the labelling process does not affect the protein structure both in the absence and in the presence of L-Glu.

Figure 1c and Fig. 1d show the time-dependent variations of the maximum fluorescence intensity emission of GluB and GluB-acrylodan in the absence and in the presence of L-Glu upon incubation at 50°C, respectively.

On one hand, the results confirm a negligible effect of the protein labelling on the structural stability of GluB at 50°C. On the other hand, they point out the stabilizing effect of the presence of L-Glu on the protein structure [34].

2.2 Steady-state fluorescence spectroscopy results

To evaluate the binding capacity of GluB-acrylodan, titration experiments were performed by adding increasing amounts of L-Glu to a GluB-acrylodan solution.

Figure 2 shows the fluorescence emission spectra of GluB-acrylodan upon excitation at 365 nm in the absence and in the presence of increasing amounts of L-Glu.

The results reveal a significant increase in fluorescence emission intensity and a blue-shift of the emission maximum by increasing L-Glu concentrations, suggesting a variation of the protein structure upon L-Glu binding. In particular, it is possible to hypothesize that the binding of L-Glu to GluB prompts acrylodan to move to a more hydrophobic and water-shielded micro-environment [35–37].

2.3 Time-resolved fluorescence results

To further investigate the effect of L-Glu on the GluB-acrylodan structure, time-resolved fluorescence measurements were performed.

Table 1 reports the GluB-acrylodan fluorescence decay parameters (obtained through a bi-exponential fit) in the L-Glu concentration range between 0.0 mM and 20.0 mM. The results point out an increase of values of GluB-acrylodan short and long lifetime components as well as of the mean-lifetime value, indicating that acrylodan molecules are more deeply buried in the protein matrix upon L-Glu binding.

To better visualize the time-resolved results, we analyzed the data by the lifetime distribution model.

Figure 3 (panels a-d) illustrates the fractional distribution as a function of fluorescence lifetime (τ) of GluB-acrylodan in the absence and in the presence of 2.0 mM L-Glu, 10.0 mM L-Glu and 20.0 mM L-Glu.

The addition of L-Glu causes the shift of the longer lifetime component (τ_2) from 6.14 ns to 7.55 ns. This increase suggests that the L-Glu binding induces a change in the protein structure that shields the acrylodan molecules from the aqueous environment, hiding them in a more hydrophobic position.

Figure 4 shows the variation of the GluB-acrylodan average fluorescence lifetime values as a function of L-Glu concentration. The GluB-acrylodan average fluorescence lifetime increases from 3.14 ns to 3.39 ns in the presence of 20 mM L-Glu.

To calculate the GluB-acrylodan/L-Glu dissociation constant (K_d), the experimental data were fitted using the Hill Eq. 3[8]. The results show a K_d of 0.29 mM (49.04 ng/µL) (Fig. 4).

Notably, this value is significantly higher than the value of K_d of 0.6 nM reported for the unlabeled GluB [34]. This may indicate that the acrylodan labelling process interferes to some extent with the protein function decreasing the GluB affinity towards the ligand [39]. This finding is consistent with the works of De Lorimier et al. [40] and Dietz et al. [41] that showed that the presence of extrinsic fluorescence probes on protein structure can alter the K_d values by perturbing the protein interactions.

Table 1
Fluorescence lifetime distribution of GluB-acrylodan upon titration with L-Glu dissolved in PBS. The table summarizes the fluorescence decay parameters obtained from bi-exponential discrete fits of GluB-acrylodan at increasing concentrations of L-Glu (0.0 to 20.0 mM).

[L-Glu] (mM)	Average lifetime (ns)	τ_1 (ns)	τ_2 (ns)	f_1	f_2	α_1	α_2
0.0	3.14 ± 0.05	0.564 ± 0.153	6.140 ± 1.018	0.375 ± 0.001	0.491 ± 0.073	0.691 ± 0.186	0.082 ± 0.025
2.0	3.30 ± 0.03	0.488 ± 0.444	6.110 ± 0.933	0.364 ± 0.031	0.516 ± 0.095	0.721 ± 0.339	0.087 ± 0.029
10.0	3.38 ± 0.06	0.647 ± 0.225	6.635 ± 1.054	0.377 ± 0.017	0.498 ± 0.089	0.616 ± 0.188	0.081 ± 0.028
20.0	3.39 ± 0.03	0.952 ± 0.223	7.555 ± 0.460	0.451 ± 0.124	0.388 ± 0.056	0.472 ± 0.019	0.052 ± 0.010

2.4 Validation of GluB-acrylodan in a simulated physiological matrix

To explore the potential utilization of GluB-acrylodan to measure the level of L-Glu in physiological matrices such as cerebrospinal fluid, we performed fluorescence lifetime measurements of GluB-acrylodan dissolved in an artificial solution of cerebrospinal fluid (see Material and Method section).

Table 2 shows GluB-acrylodan fluorescence decay results in the absence and in the presence of L-Glu (2.0 mM; 10.0 mM; 20.0 mM) obtained through a bi-exponential fit.

Figure 5 (panels a-d) illustrates the fractional distribution of fluorescence lifetimes of GluB-acrylodan in the absence and in the presence of L-Glu (2.0 mM; 10.0 mM; 20.0 mM).

The results show a different behavior of GluB-acrylodan in the aCSF solution if compared to the results obtained in the PBS solution (Fig. 3). This may be due to the more complex chemical composition of the aCSF solution, which contributes to limit the increase of the longer lifetime component (τ_2), which shifts from 5.22 ns to 5.67 ns.

Figure 6a shows the variation of the GluB-acrylodan average fluorescence lifetime as a function of L-Glu concentration. The average fluorescence lifetime values decrease from 3.05 ns in the absence of L-Glu to 2.87 ns in the presence of 20 mM of L-Glu.

The data, fitted using the Hill1 model (38), yielding a value of K_d of 3.13 mM (529.32 ng/µL) (Fig. 6a). This value is higher than the K_d of 0.29 mM calculated for GluB-acrylodan/L-Glu in PBS, probably due to the composition of the aCSF solution on the GluB-acrylodan binding event.

The specificity of the GluB-acrylodan binding assay was evaluated by testing L-serine or L-glutamine. In both cases, no fluorescence variations were registered, indicating that GluB-acrylodan does not bind these two amino acids.

Finally, the LoD was calculated by focusing on the lower concentration range of the titration curve. As depicted in Fig. 6b, a linear relationship was established between 0.0 mM and 0.1 mM L-Glu. This calibration curve was utilized to calculate the LoD using Shrivastava's method (LoD = 3.3S/b) [42], resulting in a LoD of 310 µM (52.42 ng/µL).

Table 2
Fluorescence lifetime distribution of GluB-acrylodan upon titration with L-Glu dissolved in aCSF. The table summarizes the fluorescence decay parameters obtained from bi-exponential discrete fits of GluB-acrylodan at increasing concentrations of L-Glu (0.0 to 20.0 mM).

[L-Glu] (mM)	Average lifetime (ns)	τ_1 (ns)	τ_2 (ns)	f_1	f_2	α_1	α_2
0.0	3.05 ± 0.04	0.709 ± 0.355	5.215 ± 1.068	0.365 ± 0.071	0.548 ± 0.138	0.560 ± 0.181	0.110 ± 0.049
2.0	2.96 ± 0.05	0.895 ± 0.304	5.265 ± 1.054	0.417 ± 0.048	0.502 ± 0.122	0.485 ± 0.110	0.100 ± 0.043
10.0	2.93 ± 0.01	0.851 ± 0.100	5.270 ± 0.396	0.448 ± 0.055	0.484 ± 0.016	0.526 ± 0.003	0.097 ± 0.003
20.0	2.87 ± 0.08	1.002 ± 0.267	5.665 ± 0.106	0.534 ± 0.163	0.402 ± 0.086	0.530 ± 0.021	0.071 ± 0.016

3. Conclusions

In conclusion, in this work we present the development and the validation of a fluorescence assay utilizing GluB labeled with acrylodan for monitoring the presence of L-Glu in solution.

Steady-state and time-resolved fluorescence experiments showed that L-Glu binding to the protein induces a significant conformational rearrangement in GluB-acrylodan structure. The protein binding event modifies, to some extent, the GluB-acrylodan structure, being the acrylodan molecules into a more hydrophobic protein portion as showed by the blue-shift of the steady-state emission spectra and the lifetime distribution analyses.

To demonstrate reliability in clinical applications of GluB-acrylodan, the L-Glu binding response was evaluated in a complex artificial cerebrospinal fluid (aCSF) matrix through time-resolved fluorescence experiments. The results showed a concentration-dependent decrease in the average fluorescence lifetime with a calculated LoD of 310 µM.

Since pathological L-Glu levels in neurodegenerative events can rise significantly, the detection limit of the assay is compatible with clinical applications. In conclusion, our results suggest the use of GluB as a promising tool for integration into real-time diagnostic devices, for neurobiological research, clinical monitoring, and cellular excitotoxic events.

4. Materials and Methods

4.1 Materials

All chemicals used for the preparation of the stock solutions were of analytical grade and utilized as received without further purification. Ampicillin, isopropyl β-D-1-thiogalactopyranoside (IPTG), and all chemicals used in the preparation of Luria-Bertani (LB) medium, and L-glutamine (L-Gln) were purchased from AppliChem GmbH (Darmstadt, Germany). Dimethyl sulfoxide (DMSO), L-glutamic acid (L-Glu), L-serine (L-Ser), and 1,4-Bis(5-phenyl-2-oxazolyl) benzene (POPOP) were purchased from Sigma-Aldrich (St. Louis, MO, USA). The fluorescence probe 6-acryloyl-2-dimethylaminonaphthalene (acrylodan) was obtained from Invitrogen (Eugene, Oregon, USA). For protein purification, HisTrap nickel affinity columns (GE Healthcare, Uppsala, Sweden) and PD-10 (G-25) desalting columns (Cytiva, Amersham, UK) were used.

For the preparation of artificial cerebrospinal fluid (aCSF), magnesium chloride hexahydrate ($MgCl_2$-$6H_2O$) and sodium bicarbonate ($NaHCO_3$) were purchased from AppliChem (Darmstadt, Germany). Potassium chloride (KCl) was obtained from Honeywell (Charlotte, NC, USA). Calcium chloride dihydrate ($CaCl_2 .2H_2O$) was supplied by ICN Biomedicals (Costa Mesa, CA, USA). Sodium dihydrogen phosphate (NaH_2PO_4) was purchased from J.T. Baker (Phillipsburg, NJ, USA). D-Glucose was purchased from Sigma-Aldrich (St. Louis, MO, USA). Ultrapure water was used for all solution preparations.

4.2 GluB expression and purification

The GluB protein was purified following the method described by Kronemeyer et al. [43]. GluB was expressed in *E. coli* BL21 (DE3) cells transformed with pET22b (+)-GluB, grown in LB medium containing ampicillin (50 µg/mL), and induced with 0.8 mM IPTG at 22°C overnight. Harvested cells were lysed at 20 KPSI using a Constant Cell Disruptor (Constant Systems Ltd, Daventry, UK) and treated with lysozyme (1 mg/mL), DNase (0.05 mg/mL), and $MgCl_2$ (5 mM). The lysate was purified by nickel affinity chromatography on a HisTrap column using an imidazole gradient elution. GluB-containing fractions were identified by Sodium Dodecyl Sulfate PolyAcrylamide Gel Electrophoresis (SDS-PAGE) and concentrated and further purified by size exclusion chromatography on a Superdex 75 column equilibrated with PBS (pH 7.4). Finally, the purity was evaluated by SDS-PAGE, and GluB concentration was determined by absorption spectroscopy at 280 nm.

4.3 GluB labeling and spectroscopy characterization

The labeling of GluB with acrylodan was performed as reported by Hibbs et al. [44]. Briefly, a solution of GluB 20 μM was reacted with 100 μM of an acrylodan solution (dissolved in DMSO) in a total volume of 100 μL (protein: dye molar ratio of 1:5). The reaction was incubated for 1.0 h at 25°C in the dark condition. Then, the labeled protein was purified from the unreacted dye using a PD-10 (G-25) desalting column (Cytiva, Amersham, UK) equilibrated with phosphate-buffered saline solution (PBS), pH 7.4. The elution fractions were monitored using a Jasco V-550 spectrophotometer equipped with a TrayCell (Hellma Analytics, Müllheim, Germany) by measuring the absorbance at 280 nm.

4.4 Steady-state fluorescence experiments

Steady-state fluorescence measurements were performed at 25°C on a Jasco FP-8200 spectrophotometer (Jasco, Tokyo, Japan) with a scan speed set at 500 nm/min, and excitation and emission bandwidths fixed at 2.5 nm and 10 nm, respectively. For the measurements, three different excitation wavelengths were used: 280 nm to excite the aromatic amino acids, 295 nm to excite selectively the tryptophan residues and 365 nm to excite acrylodan. The emission spectra were recorded from 310 nm to 500 nm for the first and second excitation setup and from 400 nm to 600 nm for the third one. For each experiment, the spectra of the buffer solution (PBS, pH 7.4) excited at 280 nm, 295 nm and 365 nm were acquired, and their emission contributions were subtracted from the experimental spectra. Fluorescence intensity values were mathematically corrected for dilution effects.

4.4.1 Thermal stability analysis

Thermal stability experiments were conducted on GluB and the GluB-acrylodan in the absence and in the presence of L-Glu. In particular, the two protein samples were incubated at 25°C and 50°C in sealed Eppendorf tubes and at regular time intervals (15 min, 30 min, 45 min, 60 min, 120 min, and 180 min) an aliquot of the GluB samples was analyzed by fluorescence emission measurements.

4.4.2 L-Glu titration

GluB-acrylodan binding properties were studied by fluorescence titration experiments of L-Glu (from 0.0 to 20 mM L-Glu). As a negative control, to verify thebinding specificity of GluB-acrylodan, parallel titrations of GluB-acrylodan were performed using L-Ser and L-Gln, instead of L-Glu.

4.5 Time-resolved fluorescence experiments

Time-resolved fluorescence measurements of GluB-acrylodan were performed in the absence and in the presence of L-Glu using a Chronos-ISS fluorometer (ISS, Champaign, IL, USA). A LED at 365 nm was used as the excitation source. The emission was collected through a 418 nm long pass filter to eliminate scattered light. POPOP was used as the lifetime reference standard.

The intensity decays were analyzed in terms of the multi-exponential model, through:

$$It = I_0 e^{-t/\tau} = \sum \alpha_i e^{-t/\tau} \quad (1)$$

In this equation I_0 is the intensity at t = 0, τ is the lifetime of the fluorophore, α_i are the pre-exponential factors, and $\sum \alpha_i = 1.0$.

For multi-component decays, the fractional intensity f_i of each decay time is given by:

$$f_i = \frac{\alpha_i \tau_i}{\sum \tau_i \alpha_i} (2)$$

and the average lifetime can be calculated as:

$$\tau = \sum f_i \tau_i \ (3)$$

Finally, to transition from a discrete representation to a continuous distribution, the lifetime components were transformed into continuous Gaussian profiles according to the following equation:

$$y = (\alpha \tau) e^{\left(-0.5\left(\frac{x-\tau}{0.1\tau}\right)^2\right)} \ (4)$$

4.6 Preparation of artificial cerebrospinal fluid (aCSF)

Artificial cerebrospinal fluid (aCSF) was prepared using a formulation based on established literature [45–47]. First, concentrated stock solutions were prepared by dissolving the chemical components in ultrapure water. Subsequently, a final solution was prepared by diluting these stocks to yield the final target concentrations of 140.0 mM NaCl, 2.8 mM KCl, 23.0 mM $NaHCO_3$, 1.0 mM anhydrous NaH_2PO_4, 1.2 mM $MgCl_2 \cdot 6H_2O$, 1.2 mM $CaCl_2 \cdot 2H_2O$, and 3.5 mM D-Glucose.

4.7 Data Analysis

All experimental data were processed and plotted using Origin 2018 software (OriginLab, Northampton, MA, USA). Fluorescence lifetime data were analyzed using the Vinci software (ISS Inc., Champaign, IL, USA).

To evaluate the results of GluB titration experiments, the limit of detection (LoD) was determined according to Shrivastava's approach [47] using the equation LoD = 3.3 S/b.

Declarations

Competing interests:

The authors declare that they have no known competing financial interests or personal relationships that could have appeared to influence the work reported in this paper.

Funding:

This work was funded by the European Union under the Know4Nano project, which receives funding for the Horizon Europe project under GA. No. 101159710 and ISA-CNR project Protein Sensors N. DBA.AD005.302.

Author Contribution

“Conceptualization, S. D. and M. S.; methodology, S. D. and A. V.; software, G. F. and I. M.; validation, G. F.; formal analysis G.F.; investigation G. F., A. V. and I. M.; resources S. D., M. S. and A. V.; data curation, G. F. and A. V.; writing original draft G. F. and S. D.; writing-review and editing, S. D., M. S., V. R., I. M. and A. V.; supervision, S. D. and V. R.; project administration, M. S. and S. D.; funding acquisition, S. D. All authors have read and agreed to the published version of the manuscript.”

Data Availability

The datasets used and/or analysed during the current study available from the corresponding author on reasonable request

References

1. Mutluay, S. U. & Karataş, H. A review of glutamate and its receptors: their roles in brain physiology and pathology. *Acta Med.* **53**, 99–109 (2022).
2. Zhang, D., Hua, Z. & Li, Z. The role of glutamate and glutamine metabolism and related transporters in nerve cells. *CNS Neurosci. Ther.* **30**, e14617 (2024).
3. Nicosia, N., Giovenzana, M., Misztak, P., Mingardi, J. & Musazzi, L. Glutamate-mediated excitotoxicity in the pathogenesis and treatment of neurodevelopmental and adult mental disorders. *Int. J. Mol. Sci.* **25**, 6521 (2024).
4. Kos, I. et al. Glutamate in meat processing–origin, function and novel application. *J. Cent. Eur. Agric.* **24**, 624–633 (2023).
5. Banerjee, A., Mukherjee, S. & Maji, B. K. Worldwide flavor enhancer monosodium glutamate combined with high lipid diet provokes metabolic alterations and systemic anomalies: An overview. *Toxicol. Rep.* **8**, 938–961 (2021).
6. Kazmi, Z., Fatima, I., Perveen, S. & Malik, S. S. Monosodium glutamate: Review on clinical reports. *Int. J. Food Prop.* **20**, 1807–1815 (2017).
7. Niaz, K., Zaplatic, E. & Spoor, J. Extensive use of monosodium glutamate: A threat to public health? *EXCLI J.* **17**, 273–278 (2018).

8. Cakmakci, S. & Salik, M. A. Monosodium glutamate (MSG) as a food additive and comments on its use. Proceedings of the 4th International Conference on Advanced Engineering Technologies, pp. 289–295 (2022).
9. Medina-Ceja, L., Pardo-Peña, K., Morales-Villagrán, A. & Ortega-Ibarra, J. Increase in the extracellular glutamate level during seizures and electrical stimulation determined using a high temporal resolution technique. *BMC Neurosci.* **16**, 11 (2015).
10. López-Valenzuela, C. L., Morales-Villagrán, A. & Medina-Ceja, L. A novel method for simultaneous glutamate and extracellular activity measurement in brain slices with high temporal resolution. *Talanta* **144**, 1231–1238 (2015).
11. Hamdan, S. K. & Mohd Zain, A. vivo Electrochemical Biosensor for Brain Glutamate Detection: A Mini Review. *Malaysian J. Med. Sci.* **21**, 12–26 (2014).
12. Lau, A. & Tymianski, M. Glutamate receptors, neurotoxicity and neurodegeneration. *Pflug, Arch.: Eur. J. Physiol.* **460**, 525–542 (2010).
13. Lai, T. W., Zhang, S. & Wang, Y. T. Excitotoxicity and stroke: identifying novel targets for neuroprotection. *Prog. Neurobiol.* **115**, 157–188 (2014).
14. Buckingham, S. C. et al. Glutamate release by primary brain tumors induces epileptic activity and excitotoxicity. *Nat. Med.* **17**, 1492–1498 (2011).
15. Biegański, M. & Szeliga, M. Disrupted glutamate homeostasis as a target for glioma therapy. *Pharmacol. Rep.* **76**, 1305–1317 (2024).
16. Al-Nasser, M. N., Mellor, I. R. & Carter, W. G. Is L-glutamate toxic to neurons and thereby contributes to neuronal loss and neurodegeneration? A systematic review. *Brain Sci.* **12**, 577 (2022).
17. Hou, J., Klippel, K., Bose, P. & Glutamate Excitotoxicity A Key Secondary Injury Mechanism of Traumatic Brain Injury and Spinal Cord Injury. *Front. Bioscience (Landmark Edition)*. **30**, 38904 (2025).
18. Mohan, R. D., Rajendrachari, S., Neto, H. D. A. S., Santhy, A. & Rejithamol, R. Exploration and advances in enzymatic electrochemical biosensors for in vivo detection of brain glutamate. *Bioelectrochemistry* **161**, 109161 (2025).
19. Muslim, N. Z. M., Ahmad, A., Abdullah, J. & Salam, F. Development of a sensitive biosensor for the determination of L-glutamate in food samples. *Sens. Actuators B*. **161**, 493–497 (2012).
20. Ferrara, G., Varriale, A., D'Auria, S. & Staiano, M. Shining a light on substrate affinity of glutamate-binding protein. Single-molecule insights into pH-modulated glutamate binding. *Sci. Rep.*, 1–10 (2026).
21. Hsieh, Y. H., Wang, S. S. & Chiu, T. C. Enantioselective determination of aspartate and glutamate in biological samples by ultrasonic-assisted derivatization coupled with capillary electrophoresis and linked to Alzheimer's disease progression. *J. Chromatogr. A*. **1550**, 68–74 (2018).
22. Soyseven, M. & Arli, G. Method validation and rapid determination of monosodium glutamate in various food products by HPLC–fluorescence detection and method optimization of HPLC–

evaporative light scattering detection approach without derivatization. *J. Chromatogr. Sci.* **60**, 760–769 (2022).

23. Joshi, K. M. et al. Advancing protein biosensors: redefining detection through innovations in materials, mechanisms, and applications for precision medicine and global diagnostics. *RSC Adv.* **15**, 11523–11536 (2025).
24. Erkmen, C., Taghvimi, A., Javadzadeh, Y. & Kurbanoglu, S. Sustainability of biosensors over conventional methods. RSC Detection Science 1–25 (2024) (2024).
25. Grünewald, F. S. Periplasmic binding proteins in biosensing applications. Advances in Chemical Bioanalysis, pp. 205–235 (2013).
26. Edwards, K. A. Periplasmic-binding protein-based biosensors and bioanalytical assay platforms: Advances, considerations, and strategies for optimal utility. *Talanta Open.* **3**, 100038 (2021).
27. Ausili, A., Staiano, M., Dattelbaum, J., Rossi, M. & D'Auria, S. Periplasmic binding proteins in thermophiles: characterization and potential application of an arginine-binding protein from Thermotoga maritima: a brief thermo-story. *Life* **3**, 149–160 (2013).
28. Aurilia, V., Staiano, M., Rossi, M. & D'Auria, S. New Proteins for New Sensing Methodologies: The Case of the Protein-Binding Family. Cellular and Biomolecular Recognition: Synthetic and Non-Biological Molecules, pp. 281–297 (2009).
29. Varriale, A., Marabotti, A., Mei, G., Staiano, M. & D'Auria, S. Correlation spectroscopy and molecular dynamics simulations to study the structural features of proteins. *PLoS ONE* **8**, e64840 (2013).
30. Gyimesi, G. et al. ATP hydrolysis at one of the two sites in ABC transporters initiates transport related conformational transitions. *Biochim. et Biophys. Acta (BBA) - Biomembr.* **1808**, 2954–2964 (2011).
31. Morrin, J., Petitt, C. & Abelt, C. 1,5-Acrylodan: A fluorescent bioconjugate sensor of protic environments. *Organics* **5**, 493–506 (2024).
32. Demchenko, A. P. Optimization of fluorescence response in the design of molecular biosensors. *Anal. Biochem.* **343**, 1–22 (2005).
33. Tolosa, L., Ge, X. & Rao, G. Reagentless optical sensing of glutamine using a dual-emitting glutamine-binding protein. *Anal. Biochem.* **314**, 199–205 (2003).
34. Capo, A. et al. Structural and functional characterization of the glutamate-binding protein GluB from Corynebacterium glutamicum. *Int. J. Biol. Macromol.* **162**, 903–912 (2020).
35. Qin, X., Yang, X., Du, L. & Li, M. Polarity-based fluorescence probes: properties and applications. *RSC Med. Chem.* **12**, 1100–1117 (2021).
36. Prendergast, F. G., Meyer, M., Carlson, G. L., Iida, S. & Potter, J. D. Synthesis, spectral properties, and use of 6-acryloyl-2-dimethylaminonaphthalene (Acrylodan). *J. Biol. Chem.* **258**, 7541–7544 (1983).
37. Rodrigues, F. H. S., Delgado, G. G., Costa, T. S. & Tasic, L. Applications of fluorescence spectroscopy in protein conformational changes and intermolecular contacts. *ACS Omega*. **5**, 21974–21981 (2020).

38. Lavrinenko, I. A., Vashanov, G. A., Cáceres, J. L. H. & Nechipurenko, Y. D. Fitting Parameters of a Modified Hill's Equation and Their Influence on the Shape of the Model Hemoglobin Oxygenation Curve. *Oxygen* **3**, 90–101 (2023).
39. Bobone, S. et al. Fluorescent Labeling Can Significantly Perturb Measured Binding Affinity and Selectivity of Peptide–Protein Interactions. *J. Phys. Chem. Lett.* **15**, 10252–10257 (2024).
40. de Lorimier, R. M. et al. Construction of a fluorescent biosensor family. *Protein Sci.* **11**, 2655–2675 (2002).
41. Dietz, M. S., Wehrheim, S. S., Harwardt, M. L. I., Niemann, H. H. & Heilemann, M. Competitive binding study revealing the influence of fluorophore labels on biomolecular interactions. *Nano Lett.* **19**, 8245–8249 (2019).
42. Shrivastava, A. Methods for the determination of limit of detection and limit of quantitation of the analytical methods. *Chronicles Young Scientists*. **2**, 21–25 (2011).
43. Kronemeyer, W., Peekhaus, R., Krämer, R., Sahm, H. & Eggeling, L. Structure of the gluABCD cluster encoding the glutamate uptake system of Corynebacterium glutamicum. *J. Bacteriol.* **177**, 1152–1158 (1995).
44. Hibbs, R. E., Talley, T. T. & Taylor, P. Acrylodan-conjugated cysteine side chains reveal conformational state and ligand site locations of the acetylcholine-binding protein. *J. Biol. Chem.* **279**, 28483–28491 (2004).
45. Sonuç Karaboğa, M. N. Sensitive detection of DJ-1 in artificial cerebrospinal fluid using a portable GPTMS-coordinated gold nanoparticle-based biosensor. *Biosensors* **16**, 146 (2026).
46. Zheng, W. H., Yan, C., Chen, T. & Kang, D. Z. New scheme for the preparation and use of artificial cerebrospinal fluid. *J. Physiol. Pharmacol.* **71**, 255–264 (2020).
47. Nagaeva, E., Zubarev, I. & Korpi, E. R. Electrophysiological properties of neurons: current-clamp recordings in mouse brain slices and firing-pattern analysis. *Bio-protocol* **11**, e4061 (2021).

Figures

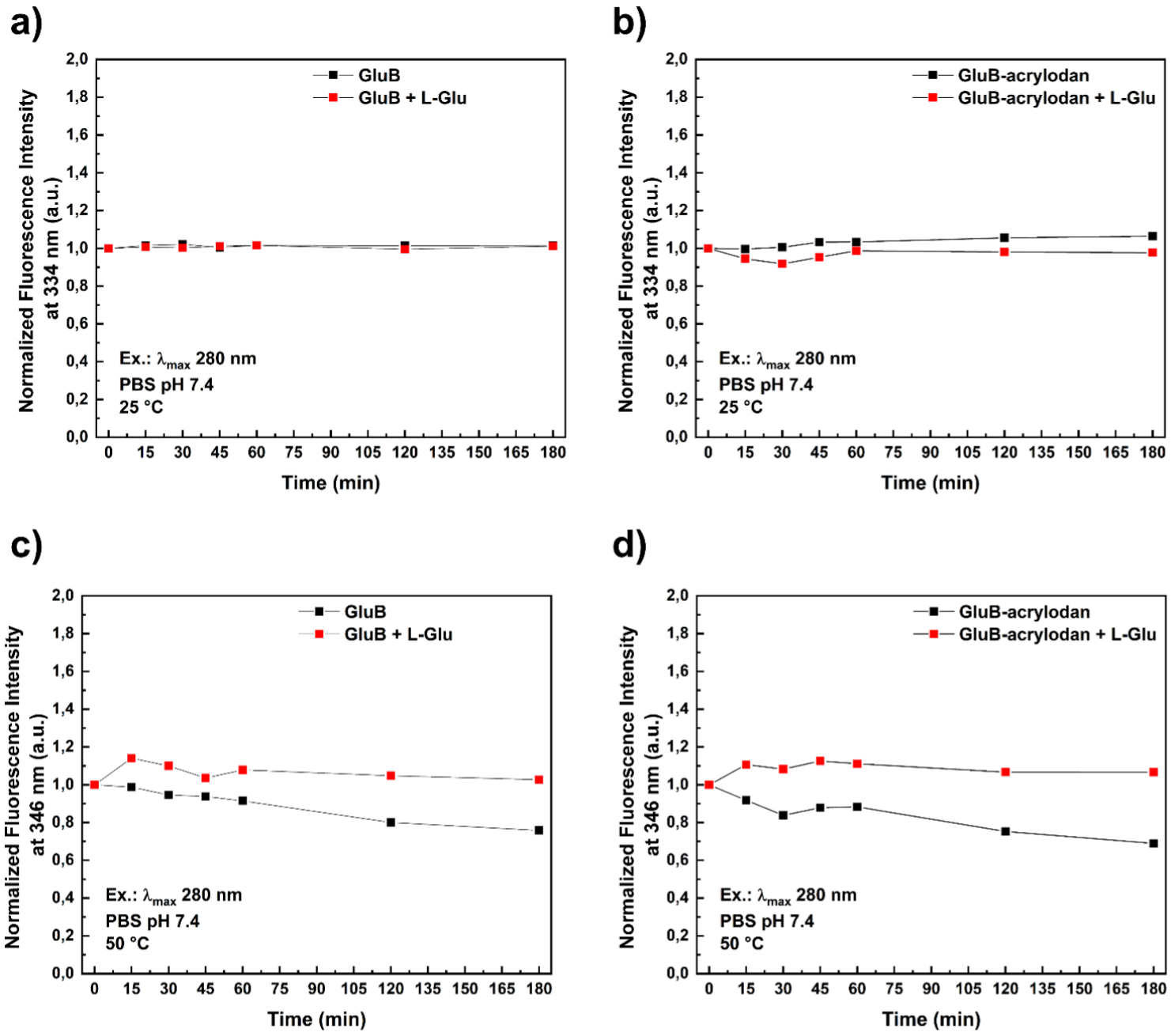


Figure 1

Thermal stability of GluB at 25 °C (a) and 50 °C (c), and of GluB-acrylodan at 25 °C (b) and 50 °C (d), in the absence (black squares) and in the presence (red squares) of L-Glu. Fluorescence emission maximum intensity was monitored over 180 min in PBS buffer (pH 7.4) upon excitation at 280 nm.

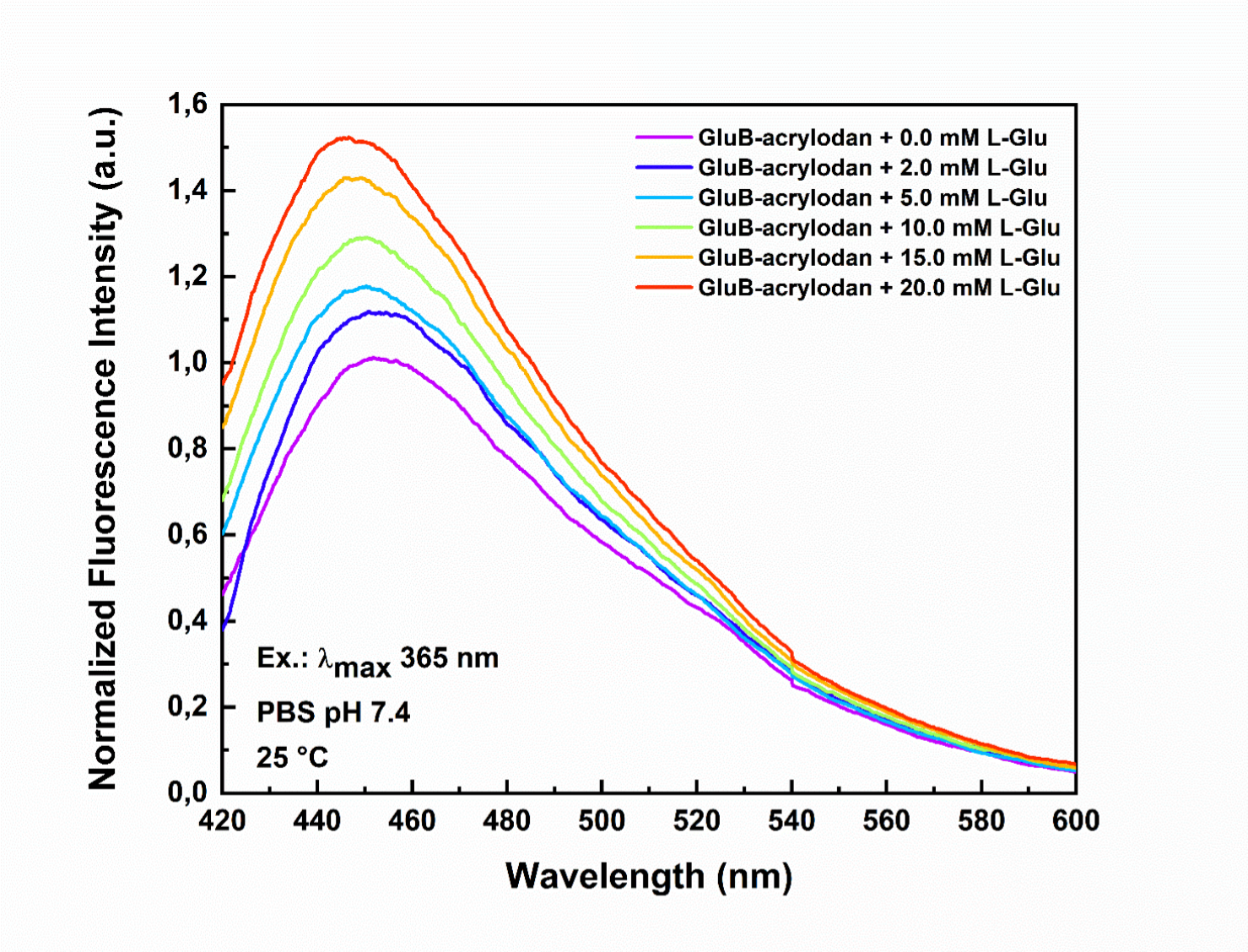


Figure 2

Steady-state fluorescence emission spectra of GluB-acrylodan in the absence and in the presence of L-Glu. The excitation value was fixed at 365 nm and the spectra were recorded at 25 °C in PBS buffer, pH 7.4. Fluorescence emission spectra at different ligand concentrations.

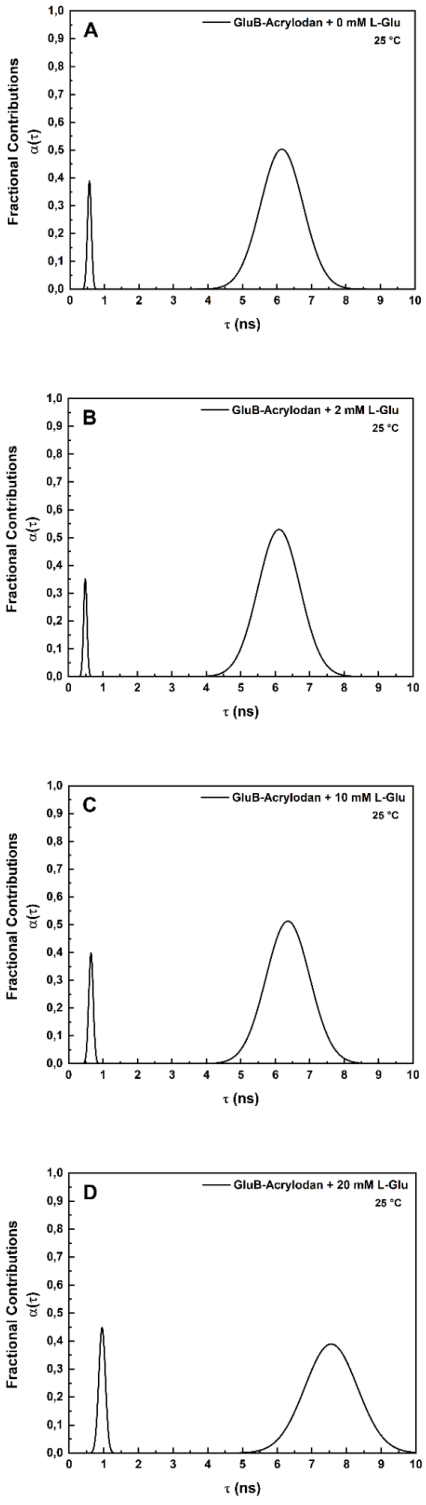


Figure 3

GluB-acrylodan fluorescence lifetime distributions at different L-Glu concentrations. The fractional contributions (α(τ)) as a function of the fluorescence lifetime (τ) for GluB-acrylodan titrated with increasing amounts of L-Glu dissolved in PBS: 0.0 mM (a), 2.0 mM (b), 10.0 mM (c), and 20.0 mM (d).

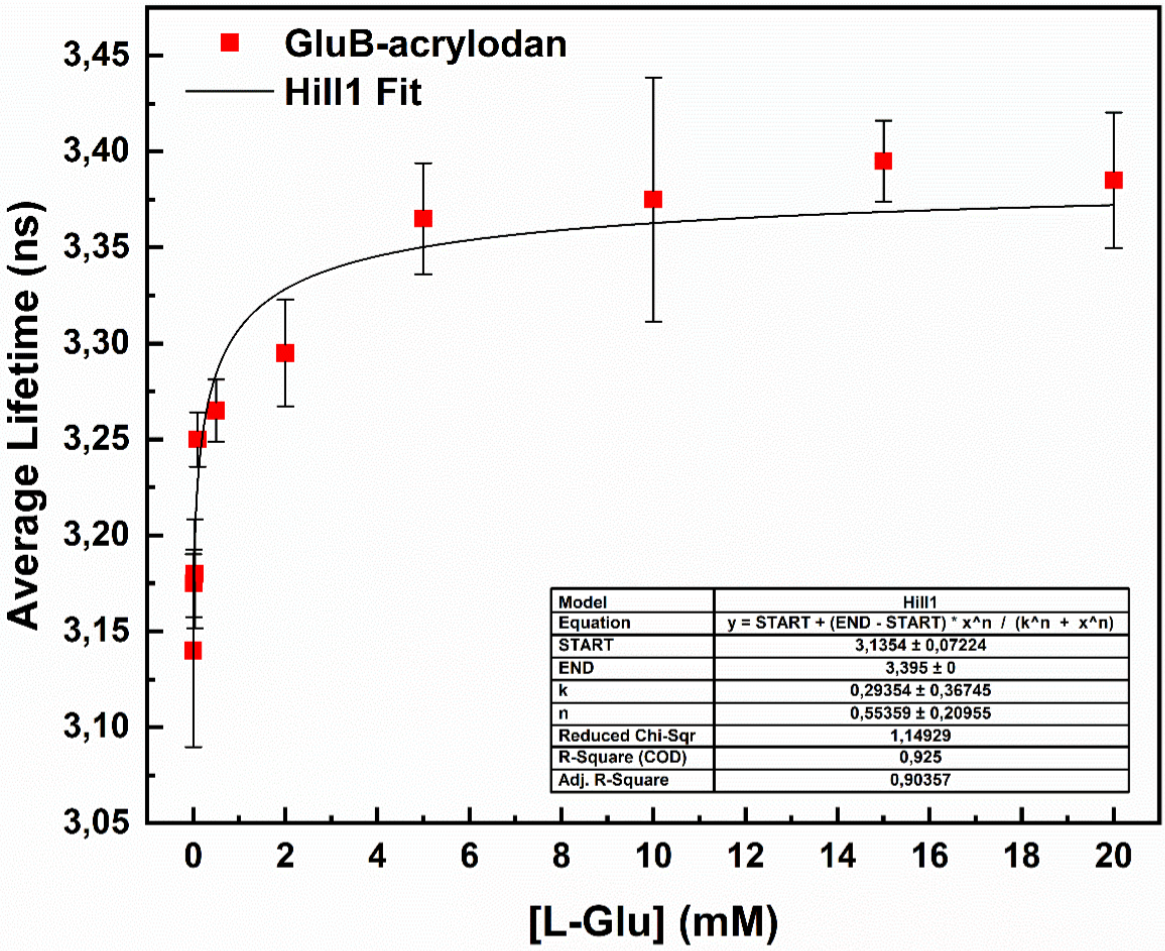


Figure 4

Time-resolved fluorescence response of GluB-acrylodan to L-Glu dissolved in PBS. Average fluorescence lifetime as a function of L-Glutamate concentration.

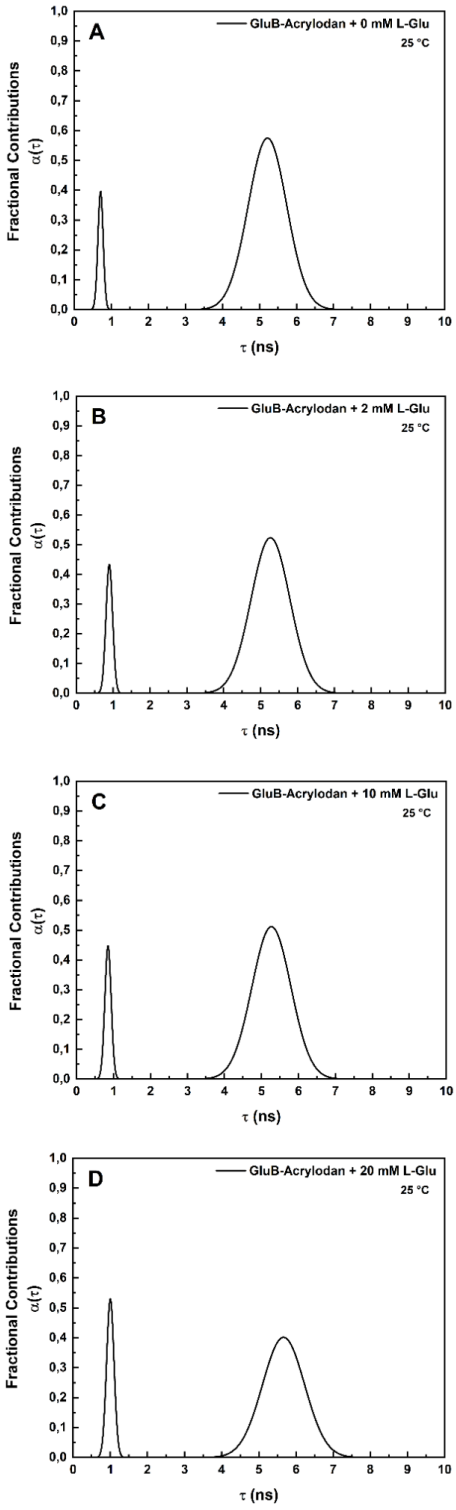


Figure 5

Fluorescence lifetime distributions of GluB-acrylodan in the absence and in the presence of 20.0 mM L-Glu. The fractional contributions (α(τ)) as a function of the fluorescence lifetime (τ) for GluB-acrylodan titrated with increasing amounts of L-Glu dissolved in aCSF: 0.0 mM (a), 2.0 mM (b), 10.0 mM (c), and 20.0 mM (d).

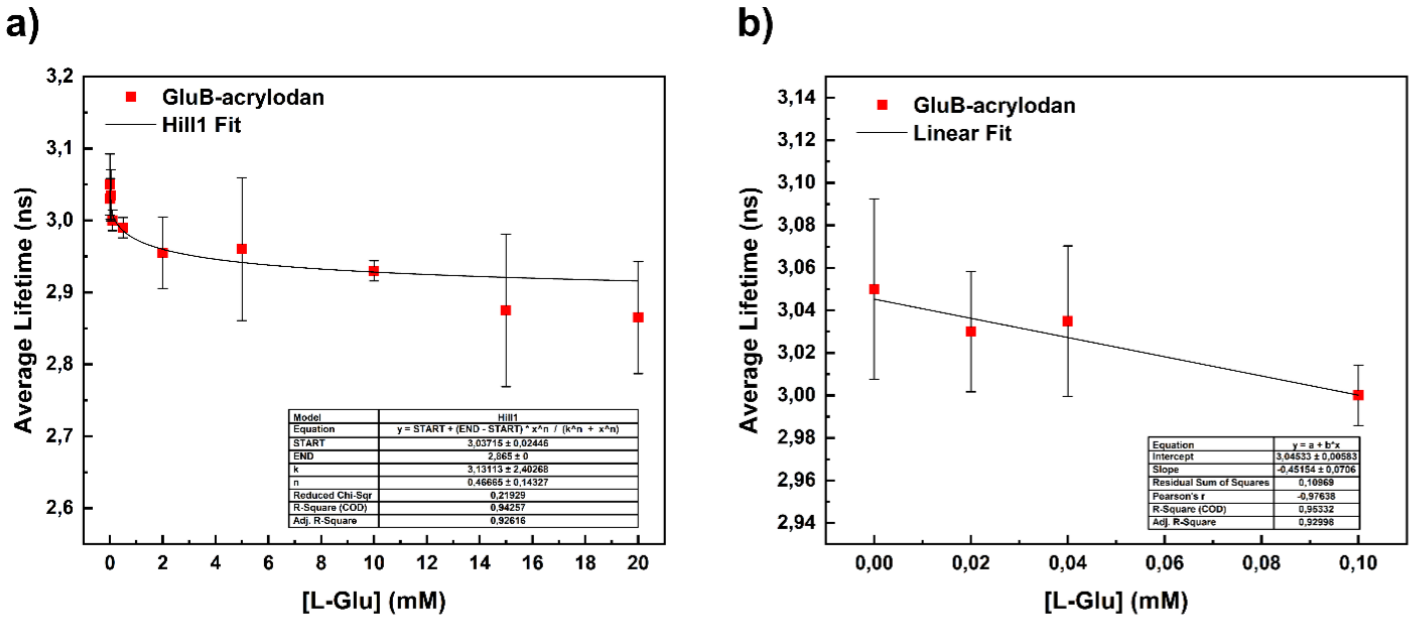


Figure 6

Time-resolved fluorescence response of GluB-acrylodan to L-Glu dissolved in aCSF. Average fluorescence lifetime as a function of L-Glutamate concentration (a) and calibration curves within the range of 0.0 mM to 0.1 mM for L-Glu (b).